Isolation and identification of pennogenin tetraglycoside from *Cestrum nocturnum* (Solanaceae) and its antifungal activity against *Fusarium kuroshium*, causal agent of Fusarium dieback

Erika Valencia-Mejía[1,†], Yeli Y. León-Wilchez[1,†], Juan L. Monribot-Villanueva[1], Mónica Ramírez-Vázquez[2,3], Israel Bonilla-Landa[4], José A. Guerrero-Analco[1,*]

[1] Laboratorio de Química de Productos Naturales, Red de Estudios Moleculares Avanzados, Instituto de Ecología A.C. (INECOL)-Clúster Científico y Tecnológico BioMimic®, Carretera Antigua a Coatepec N. 351, 91070, Xalapa, Veracruz, México.
[2] Unidad de Microscopía, Red de Estudios Moleculares Avanzados, Instituto de Ecología A.C. (INECOL)-Clúster Científico y Tecnológico BioMimic®, Carretera Antigua a Coatepec N. 351, 91070, Xalapa, Veracruz, México.
[3] Facultad de Ciencias, UNAM. Circuito Exterior, Cd. Universitaria, Copilco, Coyoacán, 04510, CDMX, México.
[4] Química Orgánica y Resonancia Magnética Nuclear, Red de Estudios Moleculares Avanzados, Instituto de Ecología A.C. (INECOL)-Clúster Científico y Tecnológico BioMimic®, Carretera Antigua a Coatepec N. 351, 91073, Xalapa, Veracruz, México.
* Correspondence: joseantonio.guerrero@inecol.mx (J.A.G-A); Tel.: +52-228-8421-800 (ext. 3514)
† Authors contributed equally to this work.

Figure S1. Mycelial growth inhibition displayed by primary fractions of *C. nocturnum* against *F. solani* at 2 mg mL^{-1}
Figure S2. Mycelial growth inhibition displayed by secondary fractions from ECn-F4 (2 mg mL^{-1}) of *C. nocturnum* against *F. solani*.
Figure S3. Mycelial growth inhibition displayed by secondary fractions from ECn-F4 (2 mg mL^{-1}) of *C. nocturnum* against *F. kuroshium*
Figure S4. Mycelial growth inhibition displayed by secondary fractions from ECn-F4 (1, 0.5 and 0.2 mg mL^{-1}) of *C. nocturnum* against *. kuroshium*.
Figure S5. ^{1}H NMR (500 MHz, Py-d5, 50 °C) of pennogenin tetraglycoside
Figure S6. Expansion from 3.0 to 7.0 ppm of ^{1}H NMR (500 MHz, Py-d5, 50 °C) of pennogenin tetraglycoside
Figure S7. Expansion from 0 to 3.2 ppm of ^{1}H NMR (500 MHz, Py-d5, 50 °C) of pennogenin tetraglycoside
Figure S8. ^{13}C NMR (125 MHz, Py-d5, 50 °C) of pennogenin tetraglycoside
Figure S9. Expansion from 60 to 115 ppm of ^{13}C NMR (125 MHz, Py-d5, 50 °C) of pennogenin tetraglycoside
Figure S10. Expansion from 0 to 60 ppm of ^{13}C NMR (125 MHz, Py-d5, 50 °C) of pennogenin tetraglycoside
Figure S11. COSY NMR (Py-d_5, 50°C) spectra of pennogenin tetraglycoside
Figure S12. TOCSY NMR (Py-d_5, 50°C) spectra of pennogenin tetraglycoside
Figure S13. HSQCed NMR (Py-d5, 50°C) spectra of pennogenin tetraglycoside
Figure S14. HMBC NMR (Py-d5, 50°C) spectra of pennogenin tetraglycoside
Figure S15. H2BC NMR (Py-d5, 50°C) spectra of pennogenin tetraglycoside
Figure S16. Stacked spectra of different TOCSY 1D at different chemical shifts of aglycone.
Figure S17. Stacked spectra of different TOCSY 1D at different chemical shifts of glycosidic portion.
Figure S18. Stacked spectra of different ROESY 1D at different chemical shifts.
Table S1. Optimized dynamic multiple reaction monitoring method (dMRM) parameters for detection and quantification of Phenolic compounds

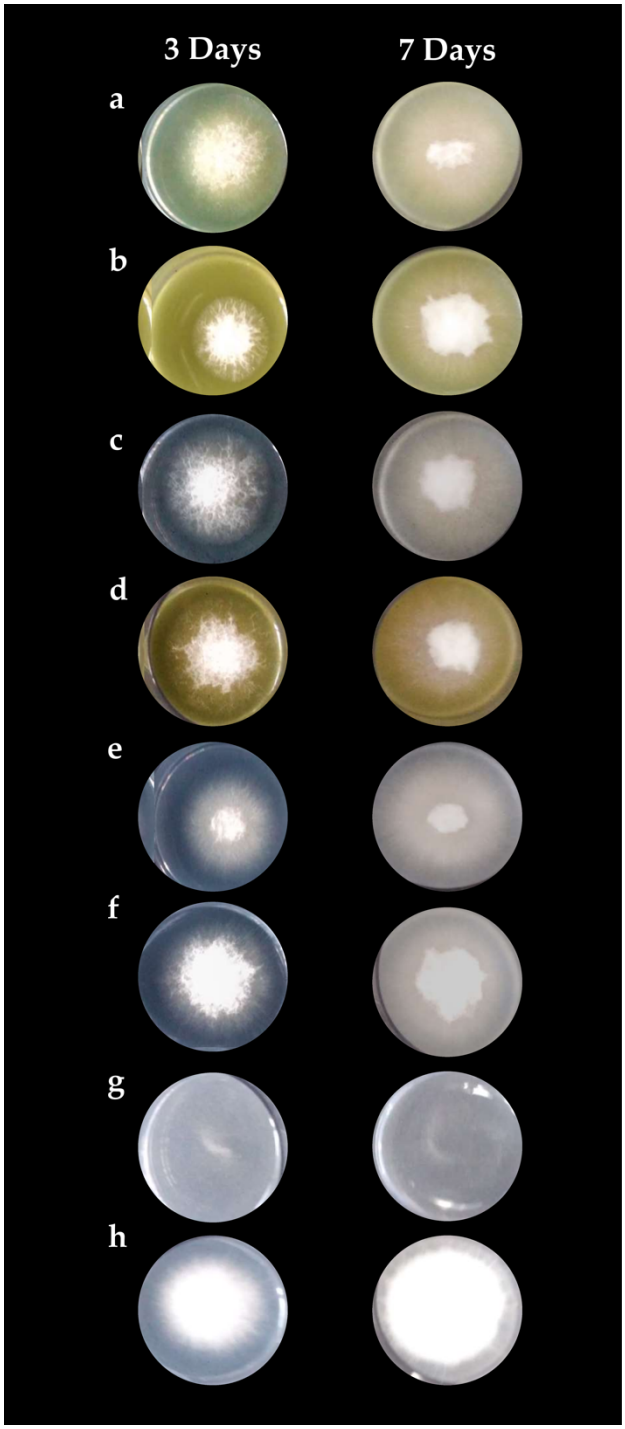


Figure S1. Mycelial growth inhibition displayed by primary fractions of *C. nocturnum* against *Fusarium solani* at 2 mg mL^{-1}, evaluated three and seven days post-inoculation. **a.** ECn; b. ECn-F1; c. ECn-F2; d. ECn-F3; e. ECn-F4; f. ECn-F5; g. Positive control (C+) thiabendazole 2 mg mL^{-1}; h. Negative control (C-) was the vehicle (H_2O-MeOH in a 15:85 ratio) where samples were dissolved.

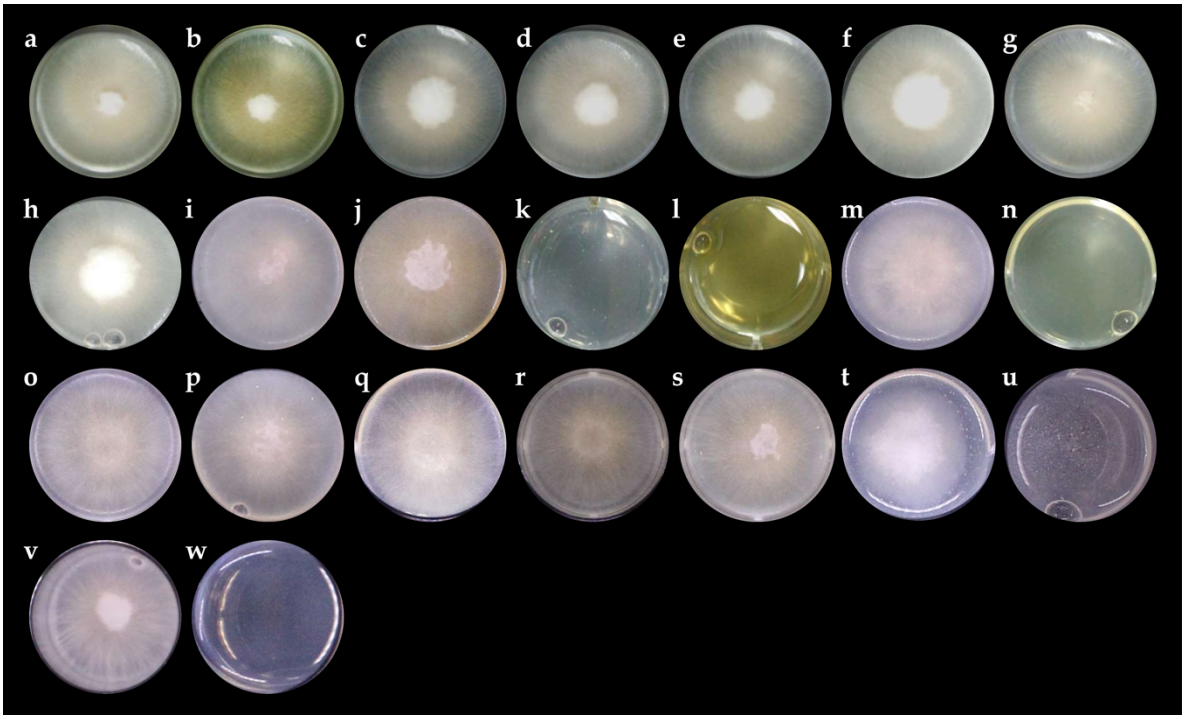


Figure S2. Mycelial growth inhibition displayed by secondary fractions from ECn-F4 (2 mg mL^{-1}) of *C. nocturnum* against *Fusarium solani*. **a.** ECn-F4-2; **b.** ECn-F4-3; **c.** ECn-F4-5; **d.** ECn-F4-6; **e.** ECn-F4-7; **f.** ECn-F4-8; **g.** ECn-F4-11; **h.** ECn-F4-13; **i.** ECn-F4-14; **j.** ECn-F4-15; **k.** ECn-F4-16; **l.** ECn-F4-17; **m.** ECn-F4-18; **n.** ECn-F4-19; **o.** ECn-F4-20; **p.** ECn-F4-21; **q.** ECn-F4-22; **r.** ECn-F4-23; **s.** ECn-F4-24; **t.** ECn-F4-25; **u.** Positive control (C+) thiabendazole 2 mg mL^{-1}; **v.** Negative control (C-) was the vehicle (H_2O-MeOH in a 15:85 ratio) where samples were dissolved; **w.** sterility control of the culture medium (PDA).

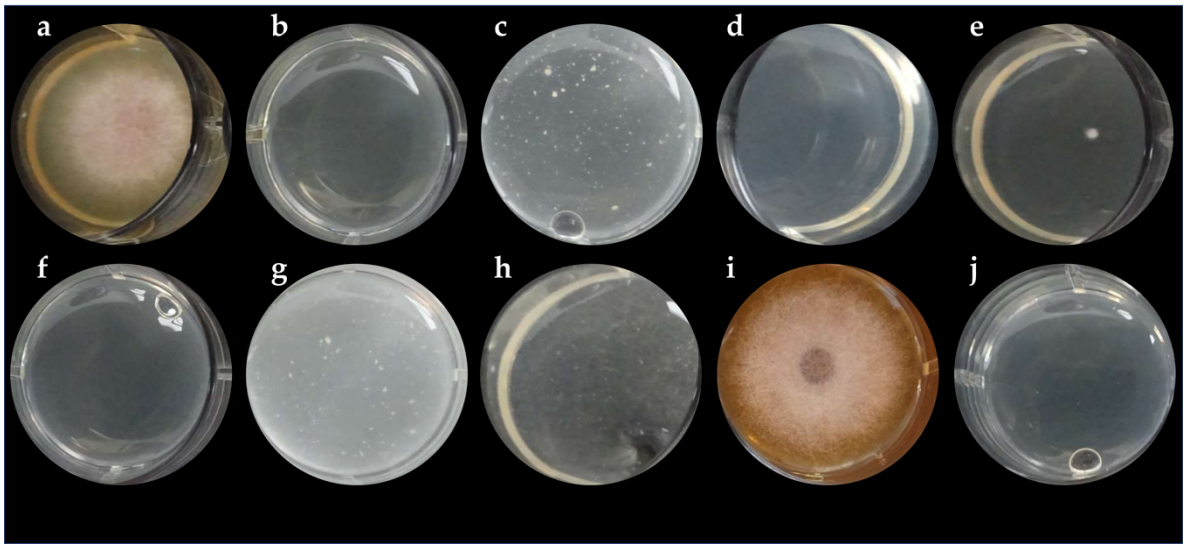


Figure S3. Mycelial growth inhibition displayed by secondary fractions from ECn-F4 (2 mg mL^{-1}) of *C. nocturnum* against *Fusarium kuroshium*. **a.** ECn-F4-3; **b.** ECn-F4-16; **c.** ECn-F4-17; **d.** ECn-F4-18; **e.** ECn-F4-19; **f.** ECn-F4-20; **g.** ECn-F4-25; **h.** Positive control (C+) thiabendazole 2 mg mL^{-1}; **i.** Negative control (C-) was the vehicle (H_2O-MeOH in a 15:85 ratio) where samples were dissolved; **j.** sterility control of the culture medium (PDA).

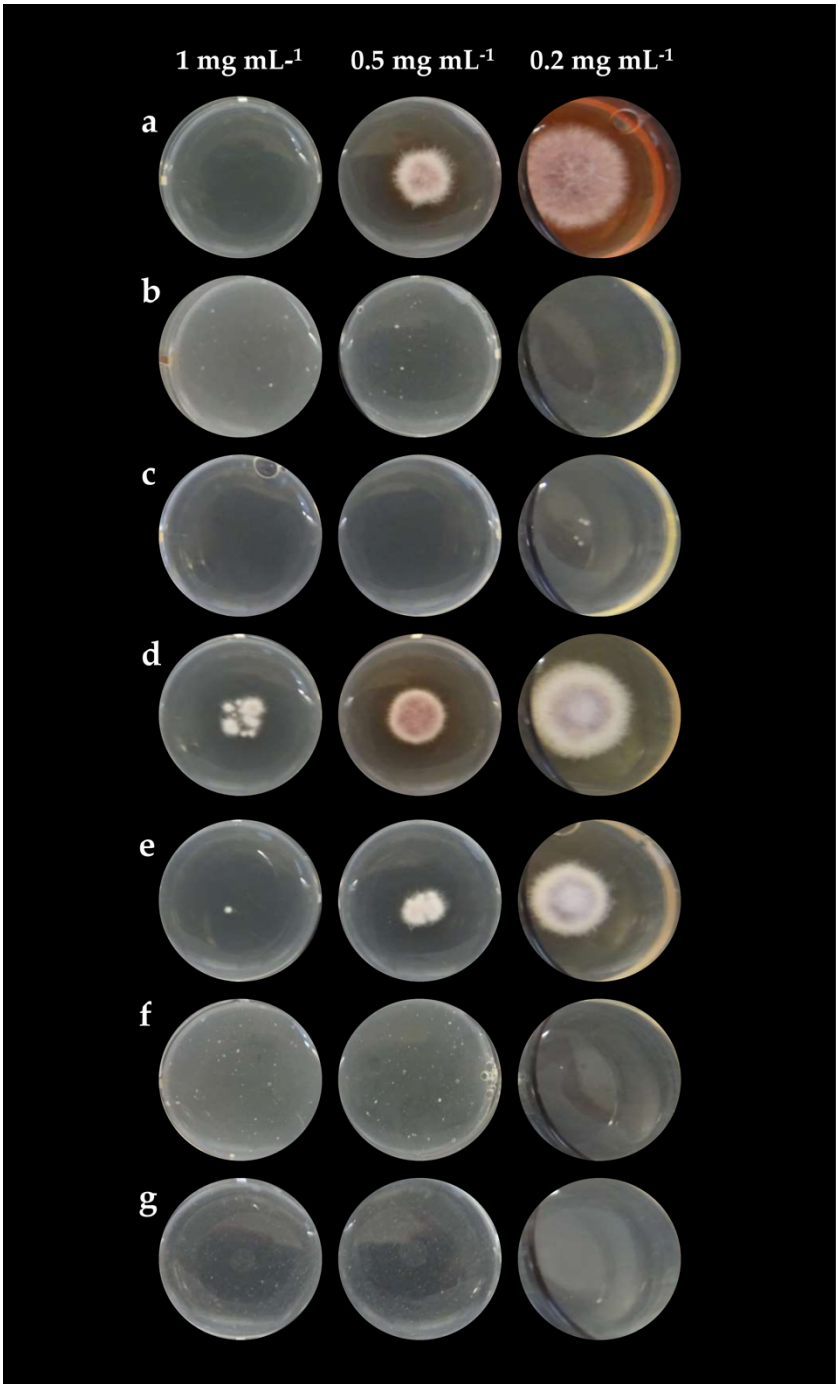


Figure S4. Mycelial growth inhibition displayed by secondary fractions from ECn-F4 (1, 0.5 and 0.2 mg mL^{-1}) of *C. nocturnum* against *Fusarium kuroshium*. **a.** ECn-F4-16; **b.** ECn-F4-17; **c.** ECn-F4-18; **d.** ECn-F4-19; **e.** ECn-F4-20; **f.** ECn-F4-25; **g.** Positive control (C+) thiabendazole at 1, 0.5 and 0.2 mg mL^{-1}.

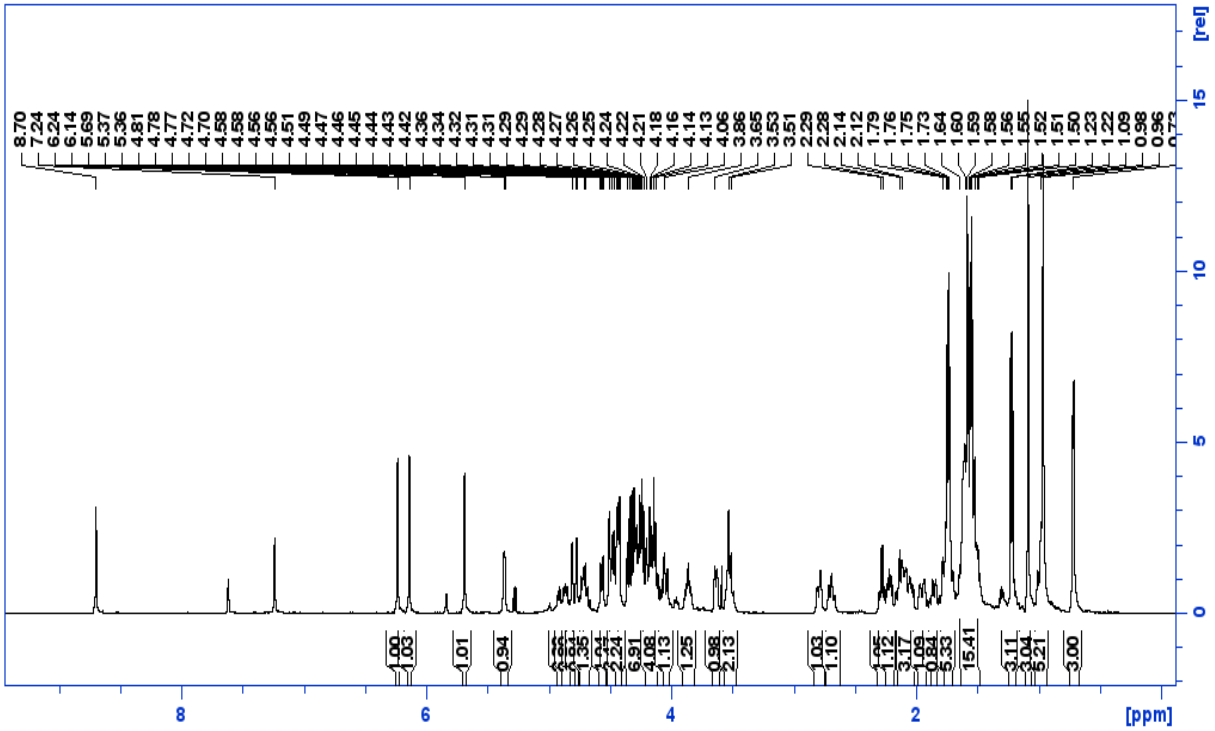


Figure S5. ^{1}H NMR (500 MHz, Py-d$_5$, 50 °C) of pennogenin tetraglycoside

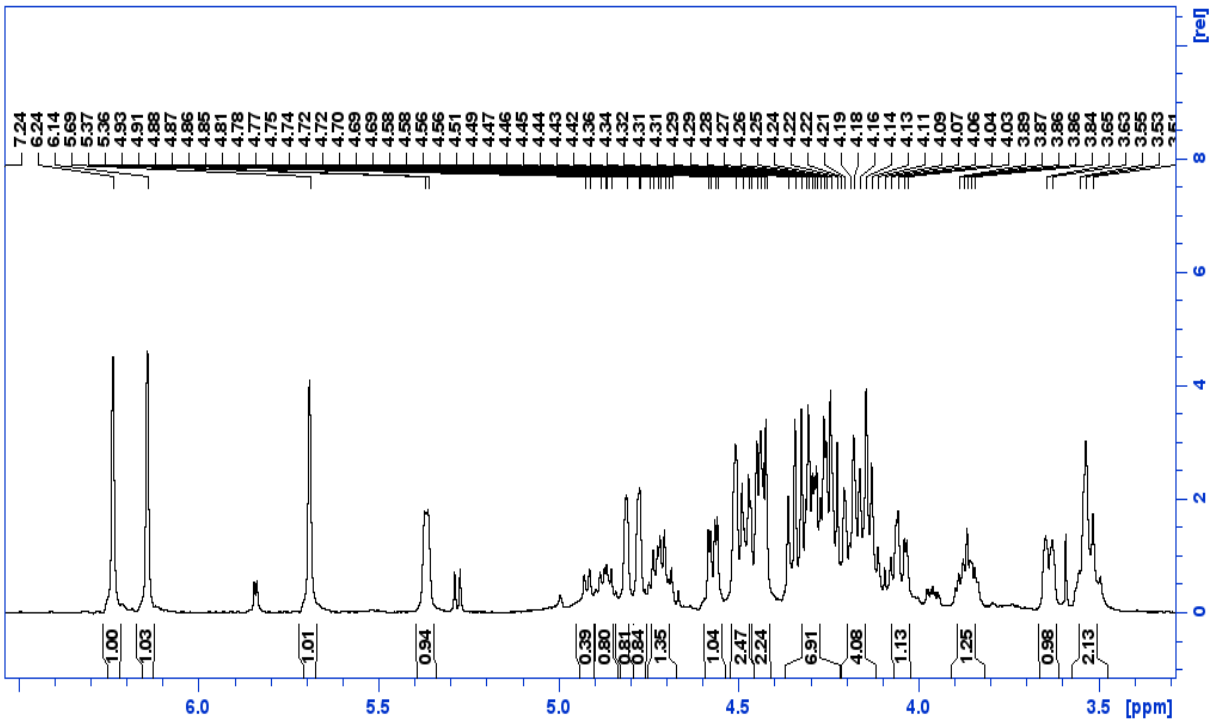


Figure S6. Expansion from 3.0 to 7.0 ppm of ^{1}H NMR (500 MHz, Py-d$_5$, 50 °C) of pennogenin tetraglycoside

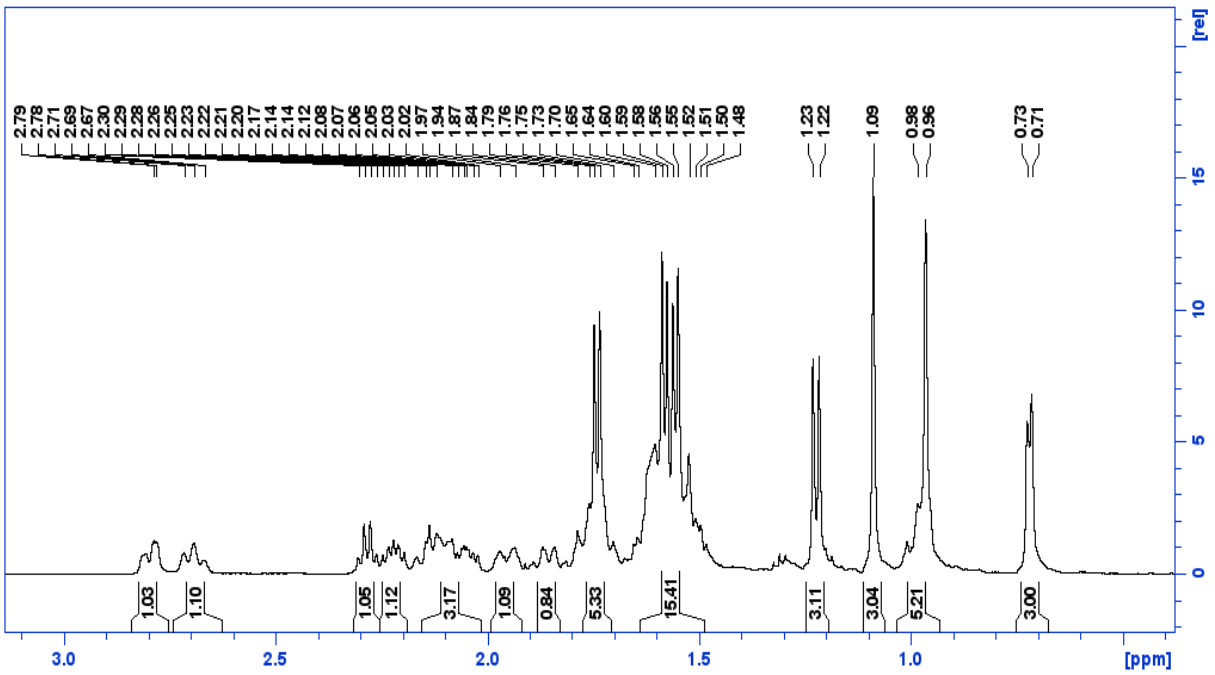


Figure S7. Expansion from 0 to 3.2 ppm of ^{1}H NMR (500 MHz, Py-d_5, 50 °C) of pennogenin tetraglycoside

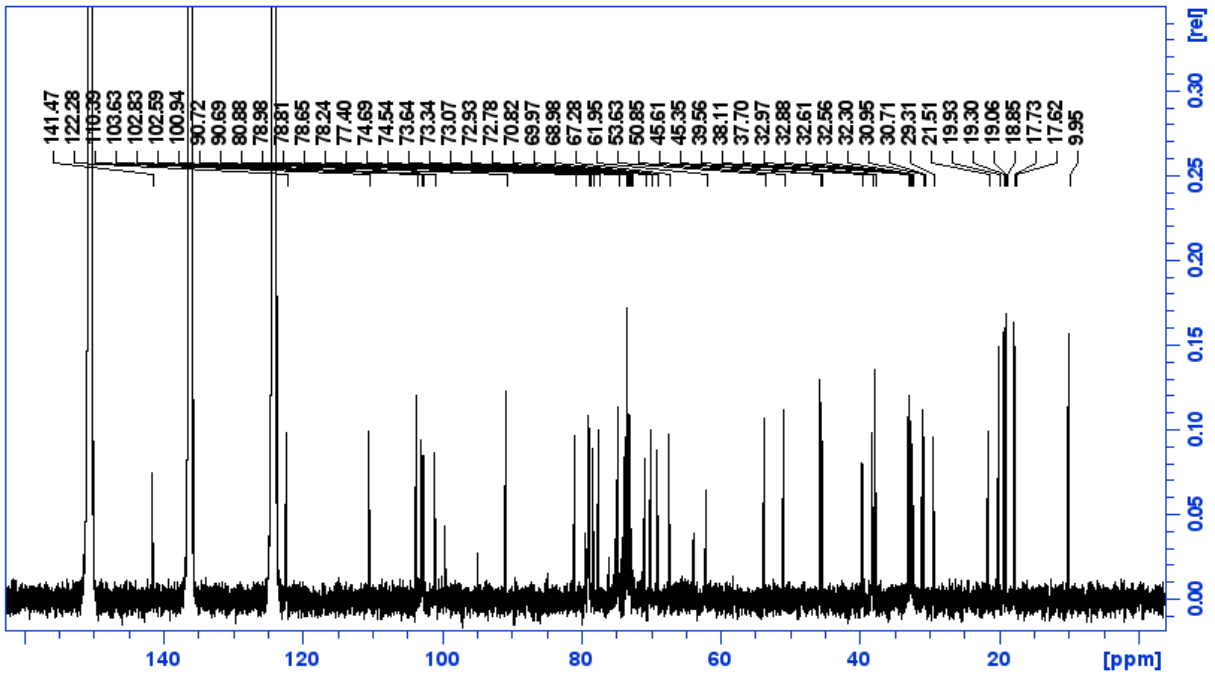


Figure S8. ^{13}C NMR (125 MHz, Py-d_5, 50 °C) of pennogenin tetraglycoside

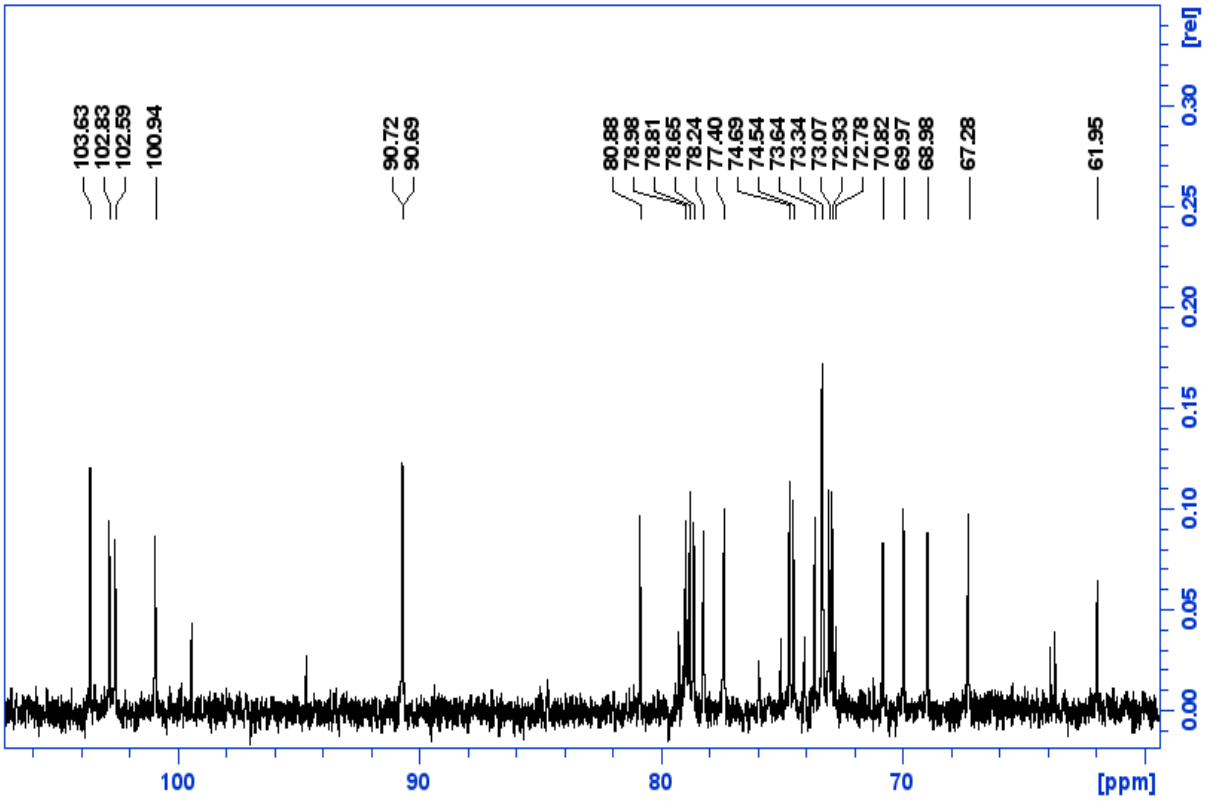


Figure S9. Expansion from 60 to 115 ppm of ^{13}C NMR (125 MHz, Py-d_5, 50 °C) of pennogenin tetraglycoside

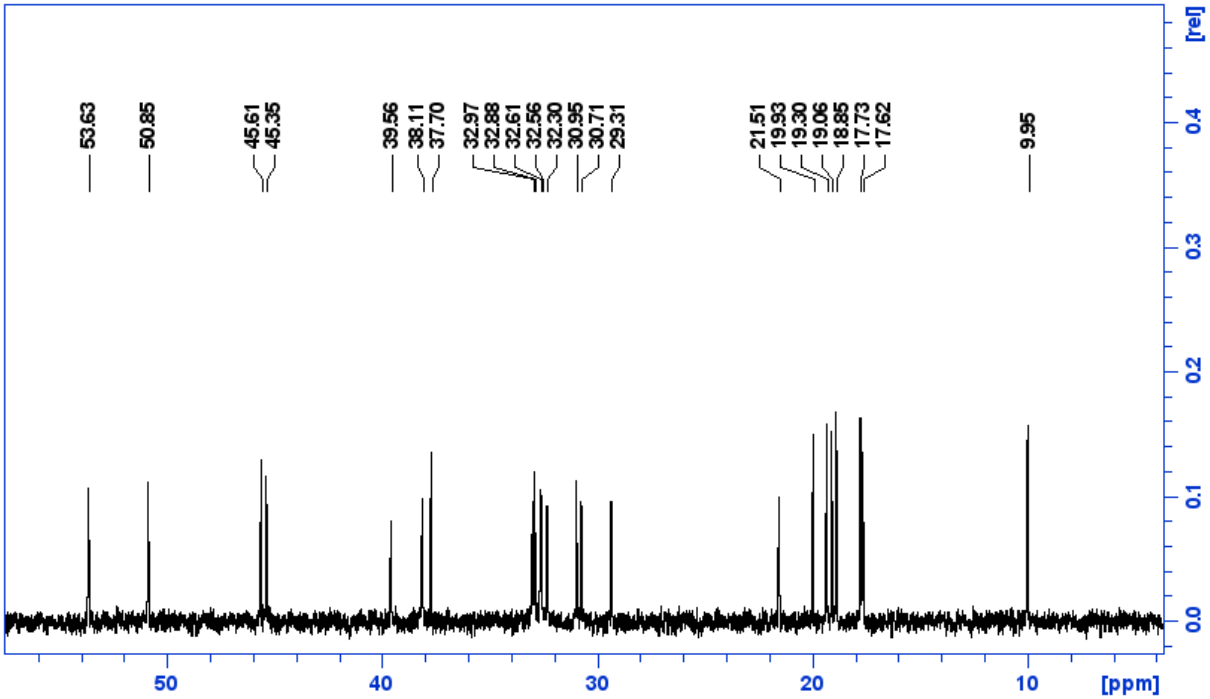


Figure S10. Expansion from 0 to 60 ppm of ^{13}C NMR (125 MHz, Py-d_5, 50 °C) of pennogenin tetraglycoside

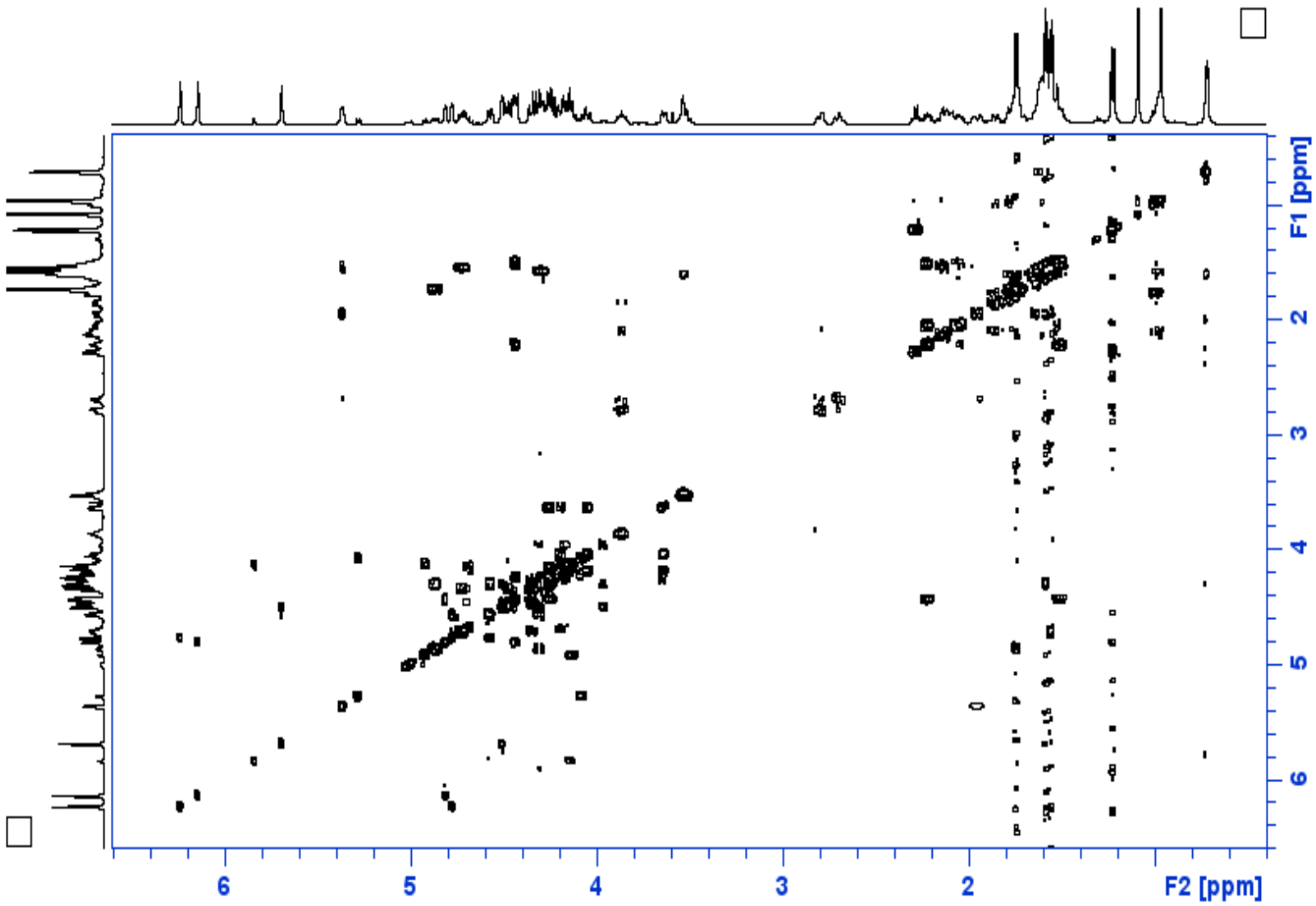


Figure S11. COSY NMR (Py-d_5, 50°C) spectra of pennogenin tetraglycoside

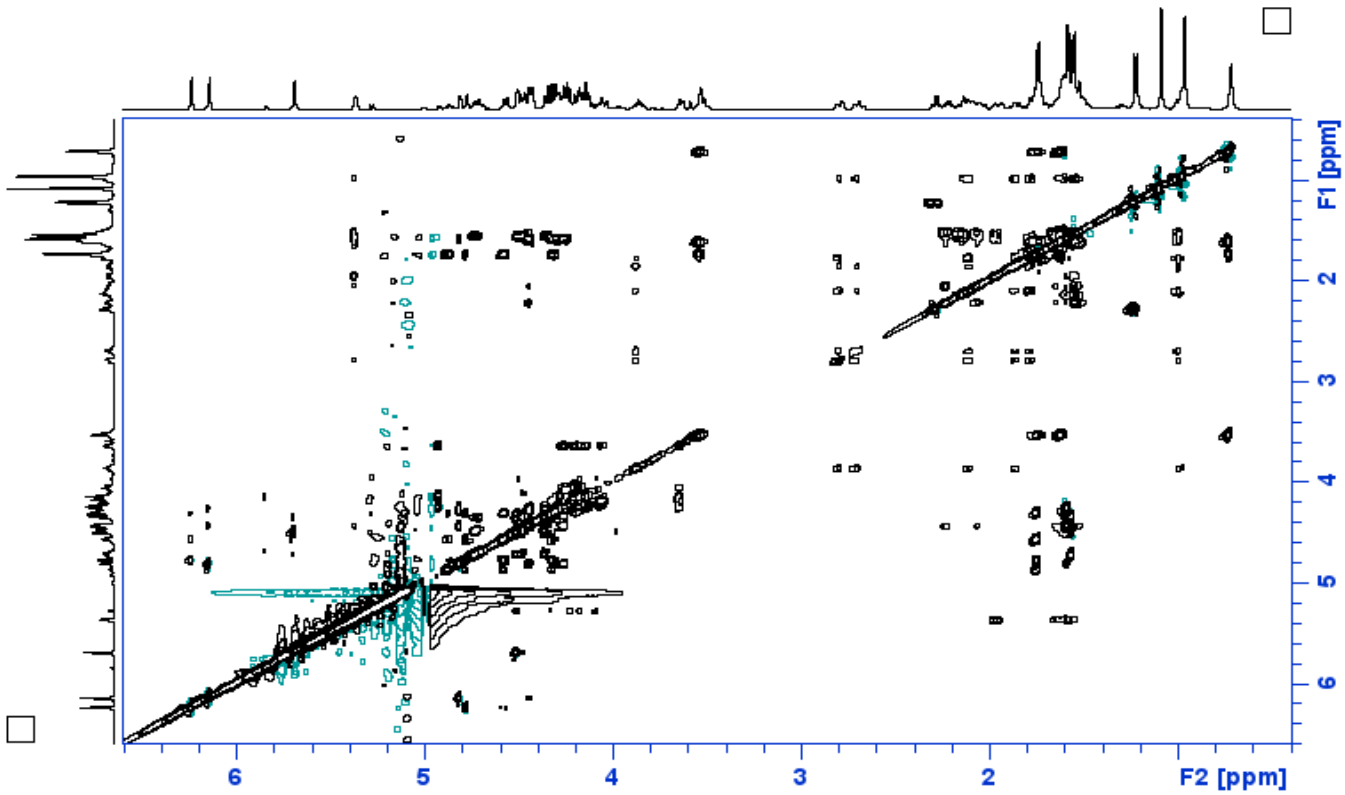


Figure S12. TOCSY NMR (Py-d_5, 50°C) spectra of pennogenin tetraglycoside

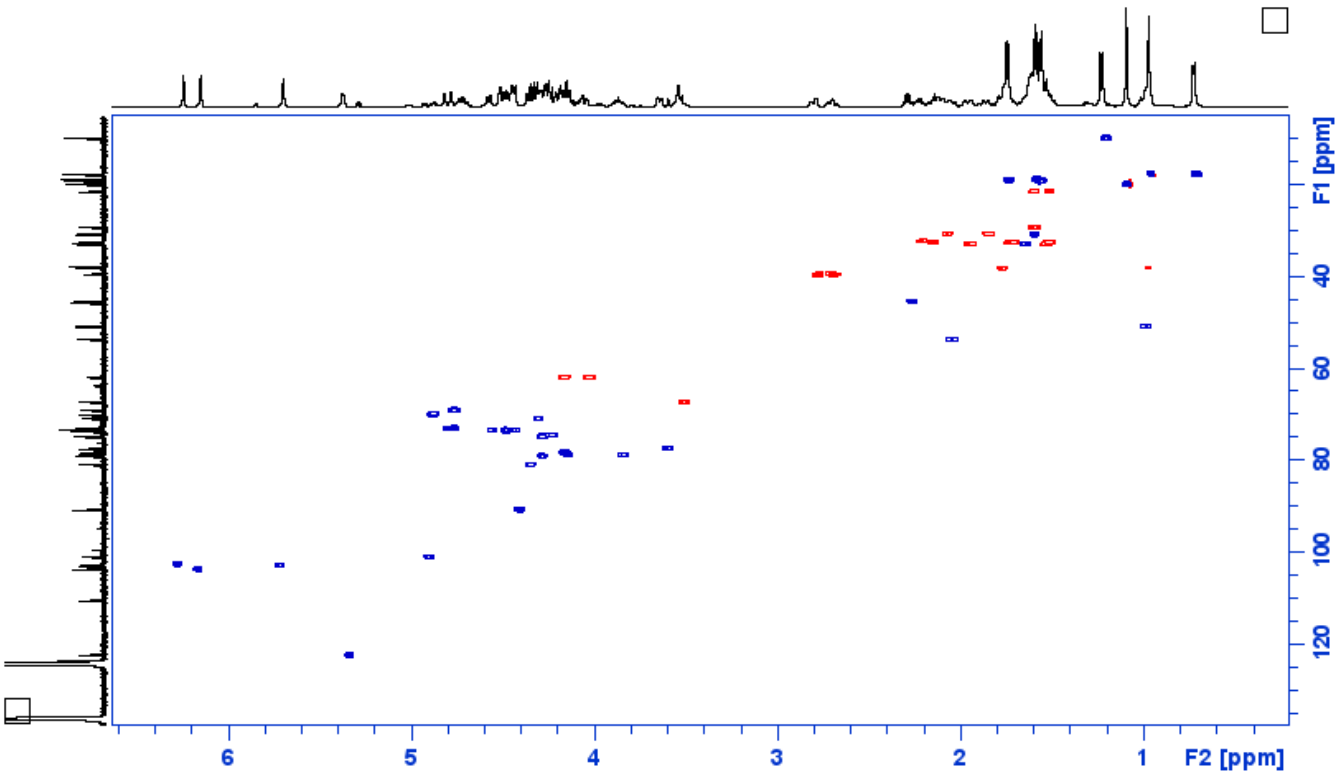


Figure S13. HSQCed NMR (Py-d5, 50°C) spectra of pennogenin tetraglycoside, blue cross peaks indicate CH and CH_3 and red cross peaks indicate CH_2

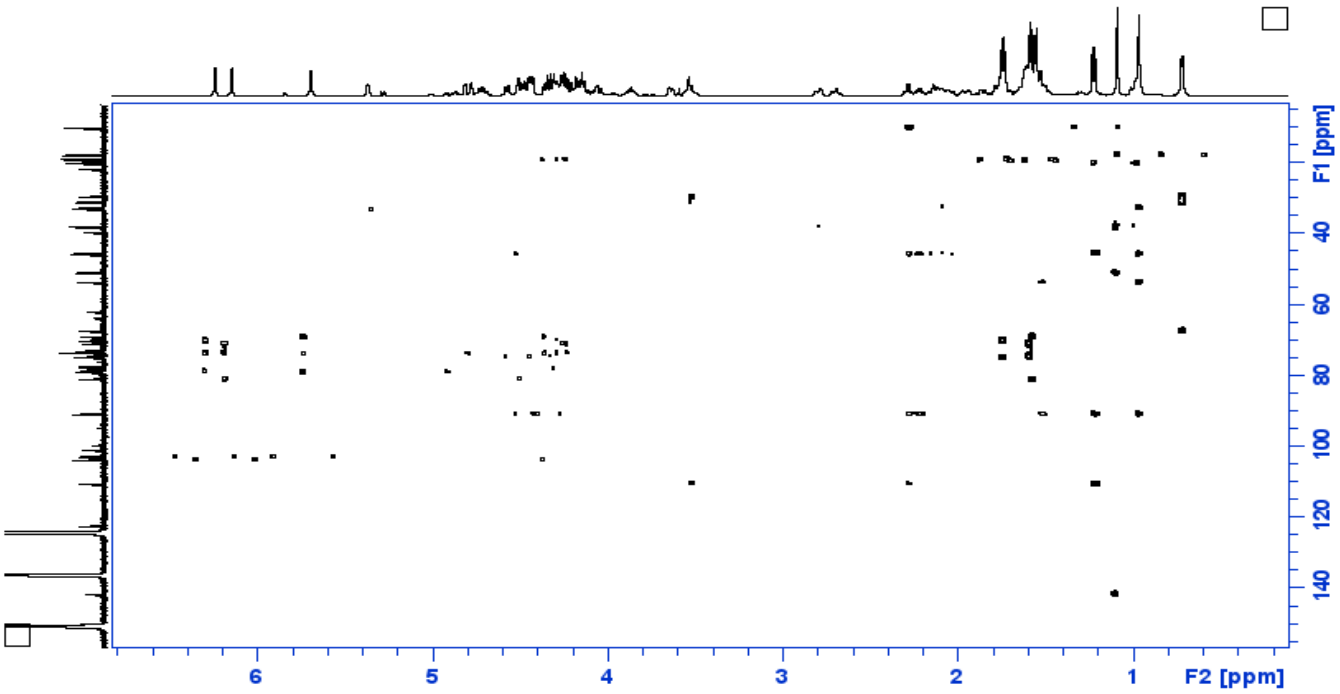


Figure S14. HMBC NMR (Py-d_5, 50°C) spectra of pennogenin tetraglycoside

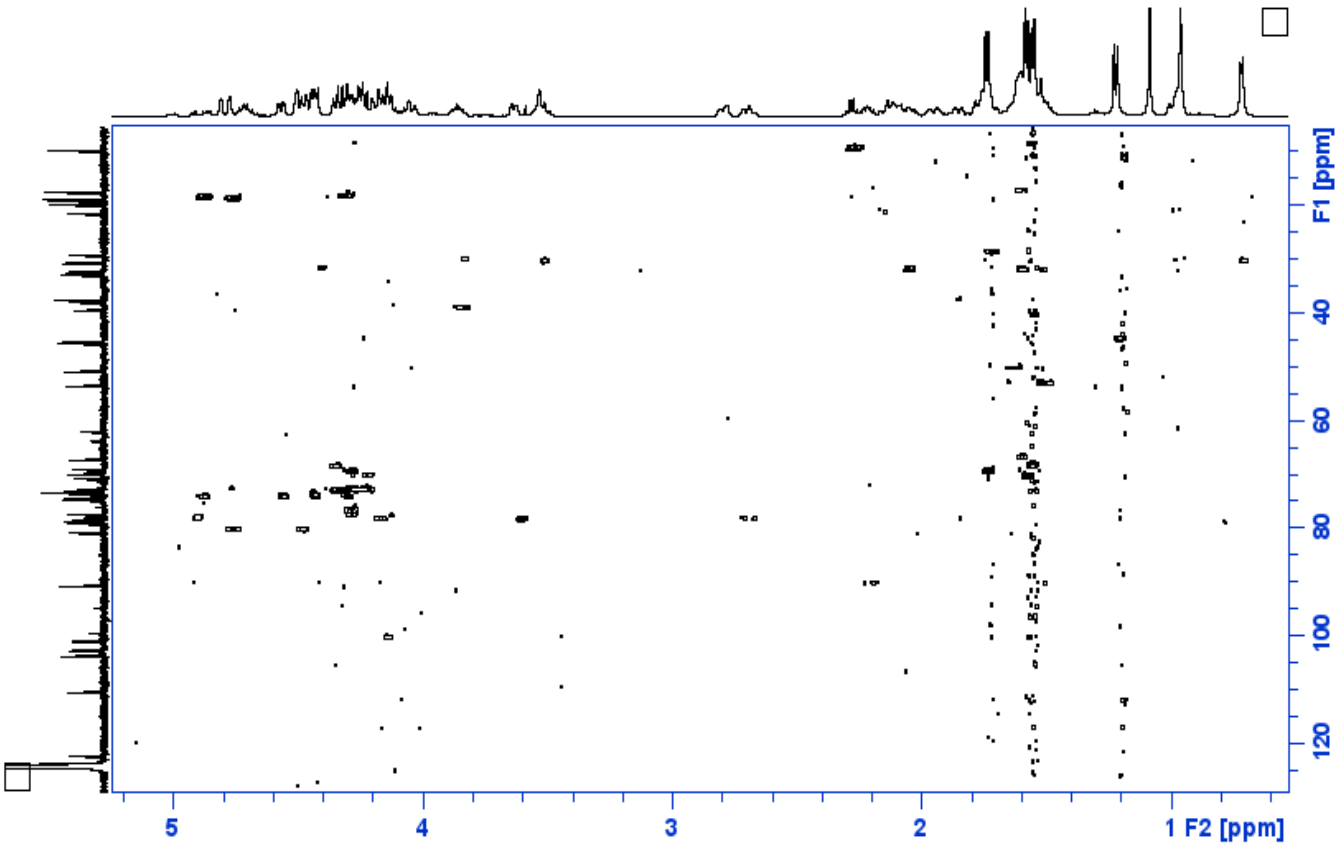


Figure S15. H2BC NMR (Py-d_5, 50°C) spectra of pennogenin tetraglycoside

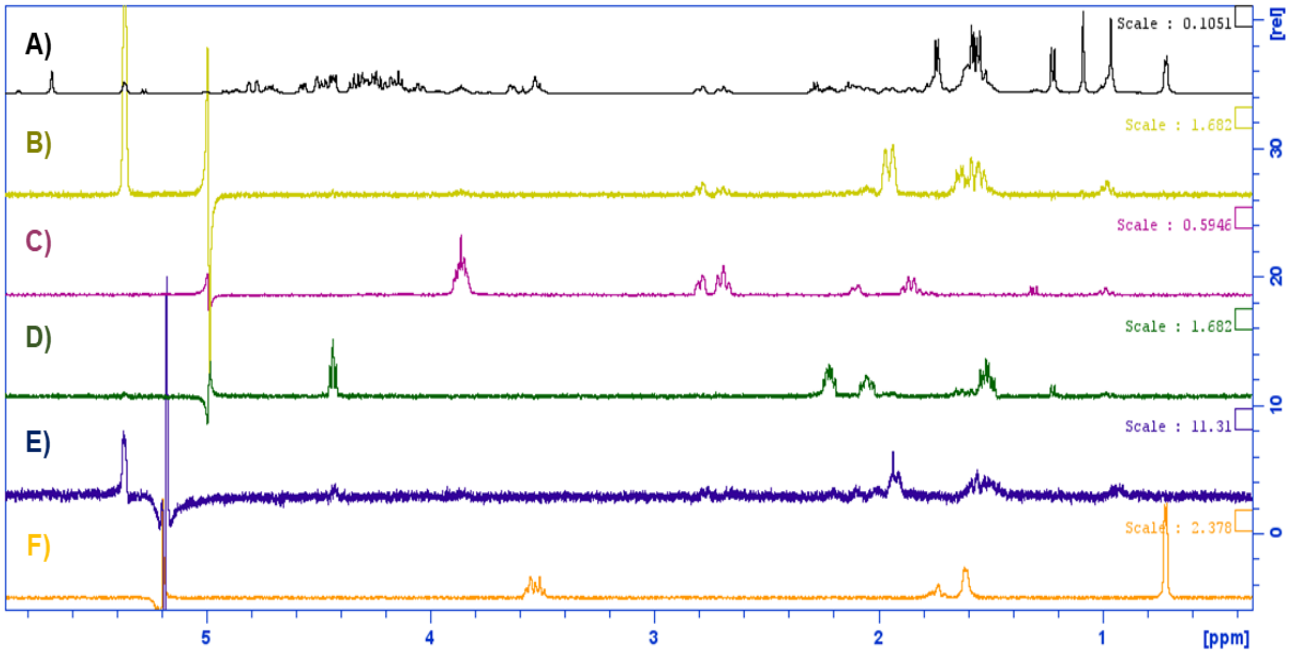


Figure S16. Stacked spectra of different TOCSY 1D at different chemical shifts of aglycone. A) ^{1}H NMR of pennogenin tetraglycoside B) Irradiation at 5.36 ppm C) Irradiation at 3.86 ppm D) Irradiation at 2.25 ppm E) Irradiation at 1.95 ppm F) Irradiation at 0.71 ppm

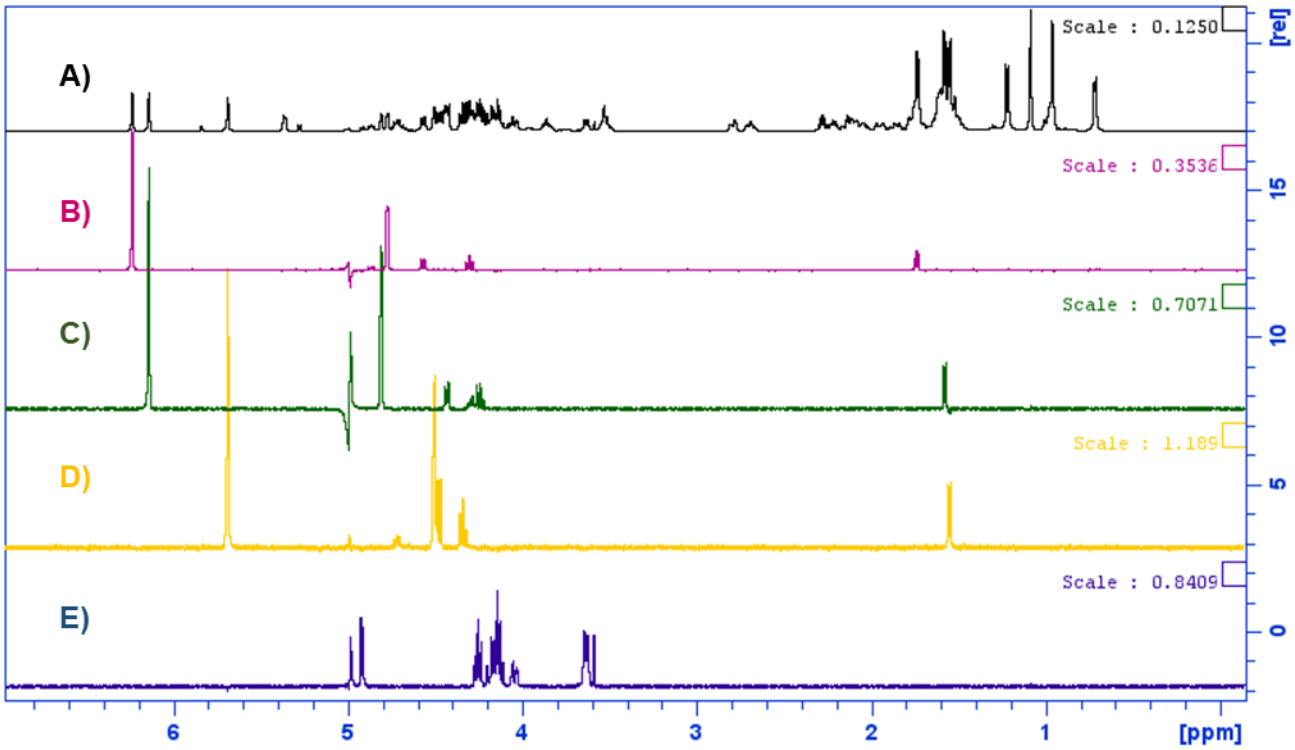


Figure S17. Stacked spectra of different TOCSY 1D at different chemical shifts of glycosidic portion. A) ^{1}H NMR of pennogenin tetraglycoside B) Irradiation at 6.23 ppm C) Irradiation at 6.14 ppm D) Irradiation at 5.69 ppm E) Irradiation at 4.92 ppm

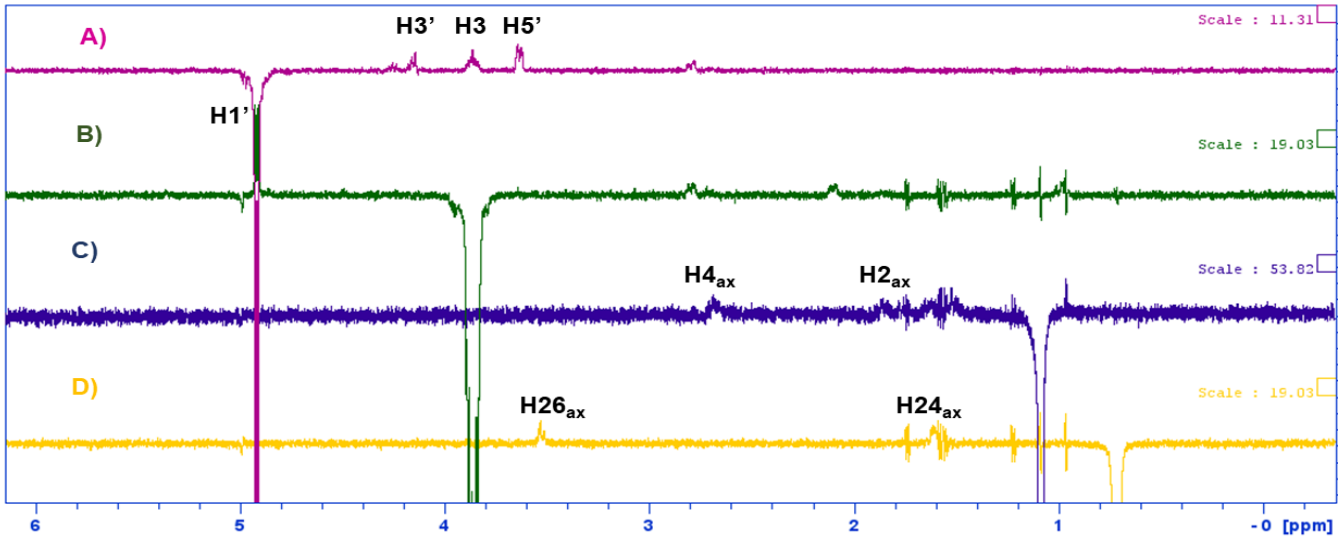


Figure S18. Stacked spectra of different ROESY 1D at different chemical shifts. A) Irradiation at 4.92 ppm proton H1' B) Irradiation at 3.86 ppm proton H3 C) Irradiation at 1.08 ppm Methyl 19 D) Irradiation at 0.71 ppm Methyl 27

Table S1. Optimized dynamic multiple reaction monitoring method (dMRM) parameters for detection and quantification of Phenolic compounds

Phenolic compound	Parent Ion (*m*/*z*)	Product Ion (*m*/*z*)	Retention Time (min)	Search Time (min)	Fragmentation Voltage (V)	Collision Voltage (V)	Polarity
Shikimic acid	173.1	111.1	1.7	0.5	100	10	-
Gallic acid	169	125.2	3.8	0.5	100	10	-
Protocatechuic acid	153	109.1	6.4	0.25	100	10	-
4-hydroxybenzoic acid	137.1	92.8	9.11	0.5	100	10	-
Gentisic acid	153	109	9.2		100	10	-
(-)-Epigallocatechin	305.1	125	10.44	0.5	100	20	-
4-Hydroxyphenylacetic acid	107.1	77	10.52	0.5	100	20	-
(+)-Catechin	291	138.9	11.2	0.5	100	10	+
Vanillic acid	169	93.03	11.81	0.5	100	10	+
Scopolin	355.1	193	11.87	0.5	100	20	+
Chlorogenic acid	355.1	163.03	12.12	0.3	100	10	+
Caffeic acid	181.04	163.03	12.24	0.5	100	10	+
Procyanidin B2	577.1	425.1	13.69	0.5	100	10	-
(-)-Epicatechin	291	138.8	14.48	0.5	100	10	+
Vanillin	153	124.9	14.99	0.5	100	10	+
Mangiferin	423	302.28	15.18	0.5	100	10	+
Keracyanin	595.2	287.1	15.2	0.5	100	20	+
4-Coumaric acid	165.05	147.04	16.22	0.25	100	10	+
(-)-Gallocatechin gallate	107	139	16.57	0.5	100	20	+
Umbelliferone	163	107	17.1	0.5	100	30	+
Quercetin-3,4′-di-O-glucoside	627	302.9	17.87	0.5	100	10	+
Scopoletin	193	133	18.44	0.5	100	10	+
3-Coumaric acid	165.05	147.04	18.7	0.5	100	10	+
Ferulic acid	195.1	145.02	19.18	0.5	100	20	+
Sinapic acid	225.1	207.1	19.57	0.5	100	10	+
(-)-Epicatechin gallate	443.1	123	19.91	0.5	100	10	+
Myricitrin	465	318.9	20.25	0.5	100	10	+
Ellagic acid	301	145	20.36	0.5	100	40	-
Quercetin-3-D-galactoside	465	302.9	20.6	0.5	100	10	-
Quercetin-3-glucoside	465	303	21.9	0.5	100	10	+
Luteolin-7-O-glucoside	449	287	21.4	0.6	100	10	+
p-Anisic acid	153.1	109	22.21	0.5	120	5	+
Penta-O-galloyl-β-D-glucose	771.1	153	22.27	0.5	100	20	+
2,4-Dimethoxy-6-methylbenzoic acid	197	179	23.43	0.5	80	5	+
Kaempferol-3-O-glucoside	449	286.9	23.64	0.5	100	10	+
Naringin	273	153	23.64	0.5	120	10	+

Quercitrin	449.1	303.1	23.71	0.5	100	10	+
Hesperidin	609.1	301.1	24.55	0.5	100	20	-
Myricetin	317	179	24.64	0.5	100	10	-
Rosmarinic acid	361.1	163	24.85	0.5	100	10	+
Phloridzin	435	272.9	25.21	0.5	100	10	-
trans-Resveratrol	229.1	135	25.86	0.5	100	10	+
trans-Cinnamic acid	149.1	131	28.5	0.5	100	10	+
Cirsimarin	477	314.9	29.4	0.5	100	10	+
Quercetin	302.9	153.1	29.7	0.5	100	35	+
Psoralen	187	131.1	31.4	0.5	100	20	+
Angelicin	187	131.1	32.74	0.5	100	20	+
Naringenin	271	151	32.83	0.5	100	10	-
Apigenin	271	153	34.1	0.5	100	30	+
Kaempferol	287.1	153	34.79	0.5	100	30	+
Hesperetin	303.1	177.1	34.8	0.5	100	20	+
Citropten	207.06	192.04	36.11	0.5	100	20	+
Nordihydroguaiaretic acid	303	193.1	42.36	0.5	100	10	+
Chrysin	255.1	153	43.13	0.5	100	40	+
Kaempferide	301	258.2	43.5	0.5	100	20	+
Emodin	269	225	44.2	0.5	150	20	-
Chrysophanol	255.1	153	45.3	0.5	100	40	+